European Journal of Medicinal Chemistry 49 (2012) 397–405

Contents lists available at SciVerse ScienceDirect

European Journal of Medicinal Chemistry

journal homepage: http://www.elsevier.com/locate/ejmech

Short communication

Synthesis, evaluation and docking studies on 3-alkoxy-4-methanesulfonamido acetophenone derivatives as non ulcerogenic anti-inflammatory agents

Alka Bali*, Ruchika Ohri, Pran Kishore Deb

University Institute of Pharmaceutical Sciences, UGC Center of Advanced Study, Panjab University, Chandigarh 160014, India

ARTICLE INFO

Article history:
Received 30 June 2011
Received in revised form
7 January 2012
Accepted 10 January 2012
Available online 18 January 2012

Keywords:
Anti-inflammatory activity
Carrageenan-induced paw edema
Docking
In silico
Field align
3D similarity

ABSTRACT

A series of 3-alkoxy-4-methanesulfonamido acetophenone derivatives were synthesized and evaluated for their anti-inflammatory activity in carrageenan-induced rat paw edema model. The synthesized compounds were also investigated for their gastric ulcerogenic potential. The compounds **4a**, **4c** and **4d** showed comparable anti-inflammatory activity to rofecoxib and indomethacin, the standard drugs taken in both studies and were also non ulcerogenic at the test doses. *In silico* (docking studies) were done to investigate the hypothetical binding mode of the target compounds to the cyclooxygenase isoenzyme (COX-2). A binding model has been proposed based on the docking studies. Selected physicochemical properties were calculated for theoretical ADME profiling of the compounds and excellent compliance was shown with Lipinski's rules.

1. Introduction

Inflammation is a protective response of our body that releases cells and mediators in order to combat foreign substances and to prevent infections [1]. Prostaglandins, produced by mast cells are the products of arachidonic acid metabolism which act as mediators and play an essential modulatory role in inflammation. Prostaglandins PGE_2, PGI_2 and PGD_2 are the powerful vasodilators in their own right and synergize with other inflammatory vasodilators, accounting for the characteristic vasodilation and erythema at the site of inflammation [2]. PGE_2 is reported to act synergistically with the primary mediators of inflammation, bradykinin and histamine producing inflammatory pain and it is considered as a principal prostaglandin for acute inflammation and chronic diseases such as rheumatoid arthritis and inflammatory bowel disease [3]. PGI_2 (prostacyclin) acts as a highly potent antithrombotic agent by inhibiting platelet aggregation (antithrombogenic effect). It is also involved in the maintenance of electrolyte balance for normal renal function in the kidneys and shows cytoprotective effect in the gastric mucosa [4–6]. Thromboxane TXA_2 found at the site of inflammation is known to have vasoconstrictive and platelet aggregative effects [4].

The term non-steroidal anti-inflammatory drugs or NSAIDs refers to a group of drugs with diverse structures of heterogeneous chemically unrelated agents, sharing common therapeutic actions and side effects. These drugs having analgesic, antipyretic (at low doses) and anti-inflammatory effects (at high doses), are usually indicated for the treatment of pain, fever and acute or chronic inflammatory diseases such as osteoarthritis, rheumatoid arthritis, dysmenorrhea and postoperative pain [7]. All NSAIDs are postulated to disrupt the biosynthesis of the prostaglandins and thromboxanes by inhibiting the enzyme cyclooxygenase [8,9]. However, inhibition of the gastrointestinal tract or renal prostaglandins results in their mechanism based toxicities manifested as gastric bleeding, life threatening gastrointestinal ulcers and on long term use it can lead to abnormal renal physiology with resultant suppression of the renal functions [10,11]. Indomethacin, ketoprofen and piroxicam appear to have highest prevalence of gastric adverse effects, while ibuprofen and diclofenac appear to have lower rates of gastric side effects [12]. Hence, the therapeutic usefulness of these potent and effective drugs gets considerably limited on account of their undesirable side effects and efforts are underway to design better anti-inflammatory drugs having lacking gastric and renal side effects.

COX-2 is the inducible form of cyclooxygenase enzyme and selective COX-2 inhibitors have been introduced in the recent years to improve upon the profile of traditional NSAIDs (t-NSAIDs).

* Corresponding author. Tel.: +91 172 2534104; fax: +91 172 541142.
E-mail addresses: alka.bali@rediffmail.com, alkaa.bali@gmail.com (A. Bali).

0223-5234/$ – see front matter © 2012 Elsevier Masson SAS. All rights reserved.
doi:10.1016/j.ejmech.2012.01.018

However, additional risks associated with several of these agents such as hepatotoxicity (nimesulide and more recently, lumiracoxib) and cardiotoxicity (rofecoxib, valdecoxib, parecoxib) has prompted their early withdrawal from the market in many countries [13]. This leaves plenty of scope for research to be carried out in this area. In this context, the present work describes the design, synthesis and the investigation of anti-inflammatory properties and ulcerogenic potential of new 3-alkoxy-4-methanesulfonamido acetophenone derivatives based on structural modification of selective COX-2 inhibitors nimesulide and flosulide. Further, a hypothetical binding model has been proposed for the compounds with respect to the target enzyme COX-2 based on *in silico* docking studies.

2. Results and discussion

2.1. Design strategy and field alignment studies

Our design strategy involved modification of the structures of known selective COX-2 inhibitors nimesulide and flosulide in order to arrive at methanesulfonamido aryl ether class of compounds (Fig. 1). Chemical structures of the prepared compounds are shown in Table 1. Structure Activity Relationship (SAR) studies on the methanesulfonamido aryl ether series of compounds (nimesulide, flosulide, etc.) have emphasized the importance of an electron withdrawing moiety at *para* position with respect to methanesulfonamido moiety for their activity [14]. Amongst these *para* substituted methanesulfonamido aryl ethers, the compounds with nitro grouping are most active followed by cyano and acetyl groups in decreasing order. Nimesulide and NS-398 contains a nitro group and Flosulide contains an indanone carbonyl as electron withdrawing functionalities. An acetyl group of acetophenone system was included as the electron withdrawing moiety in our series. The results obtained for 3D similarity are shown in Table 2. The proposed compounds showed excellent 3D similarity to flosulide (73–82%) and good similarity to nimesulide. Fig. 2 displays the near perfect alignment of **4d** (maximum 3D similarity) with flosulide molecule along with very good superposition of field points. As expected, somewhat lower values were obtained with respect to the diaryl substituted heterocycles rofecoxib and celecoxib. In all the cases, similarity values for the compounds possessing methanesulphonamido system (**4a**–**4d**) were higher than the corresponding compounds having only amino functionality (**3a**–**3d**) in the same position.

2.2. Synthesis of compounds

Synthetic scheme for the preparation of target compounds **4a**–**4d** is summarized in Fig. 3. In the first step (protection step), 2-aminophenol was refluxed with urea in presence of concentrated hydrochloric acid at 150 °C to give the cyclized product 2-(*3H*)-benzoxazolinone through a previously reported procedure [15]. Acetylation of the 2-(*3H*)-benzoxazolinone in the presence of polyphosphoric acid and acetic acid gave 6-acetyl-2-(*3H*)-benzoxazolinone **1**, which on alkaline hydrolysis yielded 4-amino-3-hydroxy acetophenone **2** in very good yields. This was followed by reaction of **2** with selected alkyl bromides employing pyridine/potassium hydroxide system to give the corresponding 1-(4-amino-3-alkoxyphenyl)ethanone derivatives **3a**–**3d**. The ether derivatives **3a**–**3d** were, then subjected to reaction with methane sulfonyl chloride affording the target compounds **4a**–**4d** in good yields (65–80%). All the reactions were standardized with respect to various reaction conditions by monitoring their progress by thin layer chromatography. The structures of the final products were authenticated and their purity ascertained by various spectroscopic techniques including UV, IR, NMR and mass spectroscopic data.

Table 1
Chemical structures of the synthesized compounds.

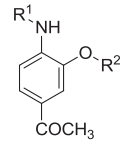

.

Compound No.	R^1	R^2
3a	H	n-C_4H_9
3b	H	n-C_5H_{11}
3c	H	n-C_6H_{13}
3d	H	cyclohexyl
4a	CH_3SO_2–	n-C_4H_9
4b	CH_3SO_2–	n-C_5H_{11}
4c	CH_3SO_2–	n-C_6H_{13}
4d	CH_3SO_2–	cyclohexyl

2.3. Pharmacological evaluation

2.3.1. In vivo anti-inflammatory studies

The prepared test compounds **3a**–**3d** and **4a**–**4d** were subjected to *in vivo* anti-inflammatory studies using carrageenan-induced rat paw edema model [16]. Rofecoxib and indomethacin were taken as standard drugs. Doses were selected by initial titration at different dose levels. Three dose levels were employed for the standard drugs as well as the test compounds, i.e., rofecoxib (15; 35; 45 mg/kg); indomethacin (5; 10; 15 mg/kg); test compounds (25; 50; 100 mg/kg). The standard drugs and the target compounds were suspended in the vehicle (0.5%w/v solution of carboxy methylcellulose CMC). Solution of carrageenan was prepared in 0.9% saline solution (900 mg in 100 ml of distilled water). Prior permission of the Institutional Animal Ethics Committee (IAEC), Panjab University, Chandigarh, India was obtained and all experiments were conducted according to the approved protocol. All the animals were allowed free access to food and water (*ad libidum),* in a constant light–dark cycle. The general behavior of the animals was normal during the course of the experiment. Statistical comparison of the

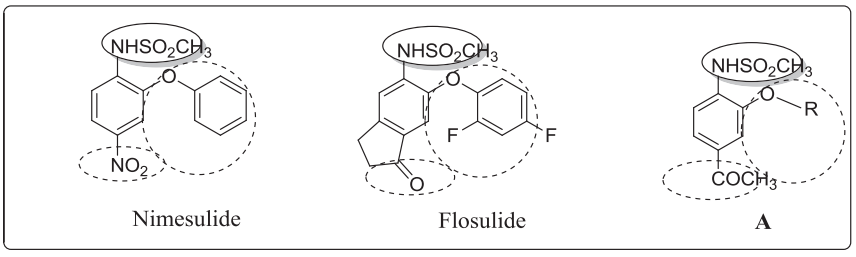

Fig. 1. Chemical structure correlation of the designed compound series (**A**) with the structures of the representative drugs.

Table 2
Three dimensional similarity of the test compounds to reference drugs.

Compound No.	Nimesulide	3D SIMILARITY Flosulide	Rofecoxib	Celecoxib
4a	0.699	0.752	0.662	0.694
4b	0.660	0.782	0.663	0.672
4c	0.649	0.728	0.658	0.677
4d	0.713	0.818	0.690	0.710
3a	0.629	0.745	0.592	0.614
3b	0.623	0.730	0.604	0.618
3c	0.619	0.737	0.613	0.631
3d	0.682	0.727	0.618	0.636

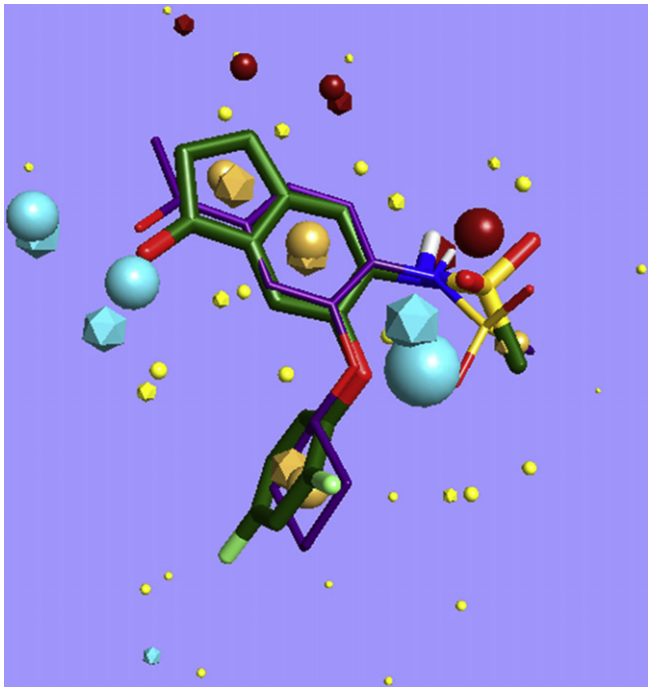

Fig. 2. Alignment of compound **4d** (thin violet sticks) with flosulide (shown as green capped sticks). Spheres, and dodecahedra depict field points for **4d** and flosulide respectively. Cyan, maroon, yellow and brown colors depict negative field, positive field, surface field and hydrophobic field points. (For interpretation of the references to colour in this figure legend, the reader is referred to the web version of this article.)

results obtained in the test groups with control and standard groups was carried out using one way ANOVA ($p < 0.001$) (Jandel Sigmastat version 2.0) followed by TUKEY test fixing the significance level at $p < 0.05$.

The results obtained for the maximum percentage edema and maximum percentage inhibition of edema in the control (carrageenan treatment), standard (rofecoxib and indomethacin) and test groups (**3a**–**3d**; **4a**–**4d**) are given in Table 3 and graphically represented in Figs. 4 and 5. The final target compounds **4a**, **4c** and **4d** were found to demonstrate good anti-inflammatory activity with the maximum reduction in edema after 5 h ranging from 72.66% to 76.75% which was comparable to those obtained for the standard drugs rofecoxib and indomethacin (81.80% and 79.74% respectively). Compound **4b** gave least reduction in paw edema. ED_{50} values were calculated for the test compounds and the standard drugs from the results of the three dose groups. Compound **4a** was found to be the most potent amongst the series and **4b** was the least potent. ED_{50} values of **4a**, **4c** and **4d** were also found to be comparable to the standard drugs (Table 3) and suggest good efficacy. In comparison, the compounds **3a**–**3d** lacking the methanesulphonamido function showed very low efficacy in the paw edema assay producing 9.88–19.02% reduction in edema after 5 h. These results further emphasize the importance of methanesulphonyl moiety for the anti-inflammatory activity of these compounds as reported for some other compound series [17,18].

2.3.2. Potential ulcerogenicity

The potential ulcerogenic effects of the compounds **3a**–**3d** and **4a**–**4d** were studied in comparison with rofecoxib and indomethacin (Table 3). None of the compounds showed any ulcerogenic effect at their highest employed doses in the three level doses studied. Only indomethacin showed red coloration, streaks and spots which increased with increase in the employed dose levels *viz*. 10, 25, 50 and 100 mg/kg.

2.4. In silico evaluation and computational studies

2.4.1. In silico (docking) studies

Docking (*in silico*) studies were performed on the compounds **4a**–**4d** as well as nimesulide found active in rat paw edema assay in order to postulate a hypothetical binding model for their interaction with COX-2 isoenzyme using the X-ray crystal structure of COX-2 (PDB ID: 1CX2). To investigate the ability of molecular

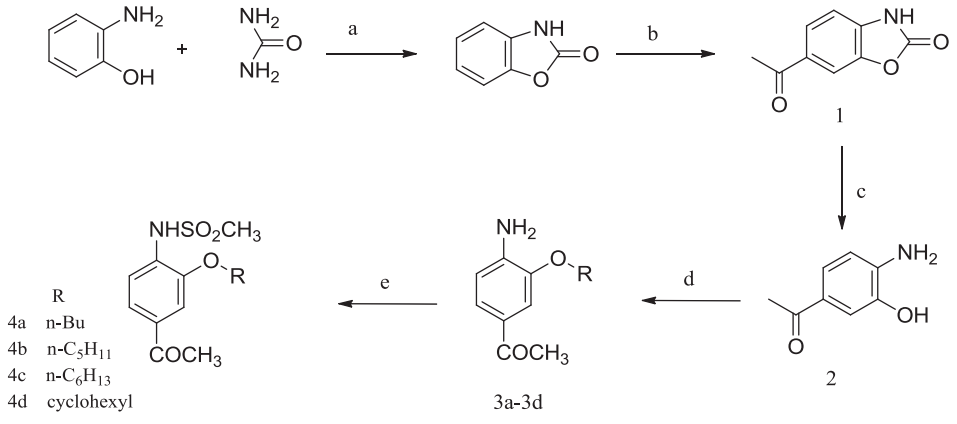

Reagents and conditions: (a) conc. HCl, 150^{0}C, reflux (b) Polyphosphoric acid, glacial acetic acid, heat
(c) NaOH, ethanol/water (d) alkyl bromide, pyridine, KOH, dichloromethane (e) CH_3SO_2Cl, pyridine,CH_2Cl_2

Fig. 3. Synthetic scheme for preparation of the target compounds.

Table 3
Results for anti-inflammatory activity and ulcerogenic potential of the tested compounds.

Treatment	Max. % edema[a]	Max. % reduction in edema from control group	ED_{50}[c] (mg/kg)	Lesion score (mm)[d]
Control	100 ± 2.73	0	_	0
Rofecoxib (30 mg/kg)	18.20 ± 2.70[b]	81.80	2.50	3
Indomethacin (10 mg/kg)	20.26 ± 54.23[b]	79.74	2.00	22.3 ± 1.45
4a	27.34 ± 2.27[b]	72.66	2.00	5
4b	40.40 ± 5.76[b]	59.60	8.18	4
4c	23.25 ± 3.13[b]	76.75	2.30	4
4d	26.35 ± 12.65[b]	73.65	2.23	3
3a	80.17 ± 13.03	13.83	–	2
3b	90.12 ± 11.79	09.88	_	2
3c	85.92 ± 12.78	14.08	_	3
3d	80.98 ± 10.73	19.02	_	3

[a] Values expressed as mean ± SEM at highest amongst the selected three dose levels after 5 h.
[b] Statistically significant vs. control ($p < 0.001$); one way ANOVA.
[c] Calculated from results for anti-inflammatory activity at three graded doses.
[d] Lesions, streaks and red spots noted at highest among the three dose levels employed.

docking to reproduce an experimentally observed ligand-binding mode, the co-crystallized ligand SC-558 (a selective COX-2 inhibitor) was used as reference ligand. SC-558 is a highly selective COX-2 inhibitor belonging to the vicinal diaryl heterocyclic class. These compounds are characterized by a central carbocyclic or heterocyclic ring system bearing two vicinal aryl moieties. For optimal activity, one aromatic ring must have a sulphonamide substituent in the para position. The two fluorines of the trifluoromethyl group ($-CF_3$) of SC-558 showed strong bonding interactions with the NH_2 group of Arg_{120} at distances of 2.86504 Å and 2.03016 Å. The same group ($-CF_3$) was also found to be located in the vicinity of amino acids Leu_{531}, Val_{116}, Leu_{359}, Val_{349} and Tyr_{355} which were within a distance of 4 Å. Further, sulphonamide $-NH_2$ was found to hydrogen bond with the nitrogen atom of imidazole ring of His_{90} at a distance of 2.50664 Å. The same $-NH_2$ group interacted with Ser_{353} and Gln_{192} at a distance of 2.84342 Å and 2.66487 Å. The sulphonamide oxygen was found to hydrogen bond with His_{90} and Arg_{513} at a distance of 2.11901 Å and 2.42782 Å respectively. The pyrazole ring of SC-558 was found in the vicinity of Val_{349} and Ala_{527}.

Further, the docking studies performed for nimesulide showed interactions with Arg_{120}, His_{90} and Arg_{513} similar to that of SC-558. The oxygen atom of methane sulfonyl group of nimesulide formed a strong hydrogen bond with $-NH_2$ of Arg_{120} at a distance of 1.62049 Å. The methanesulphonamido group interacted with Val_{349}

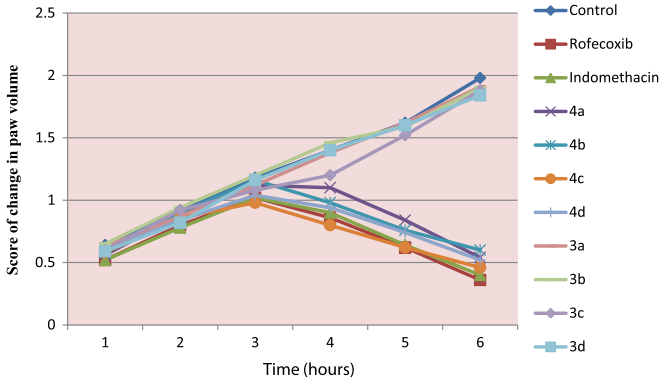

Fig. 4. Plot of mean score of change in paw volume at various time intervals for all treated groups.

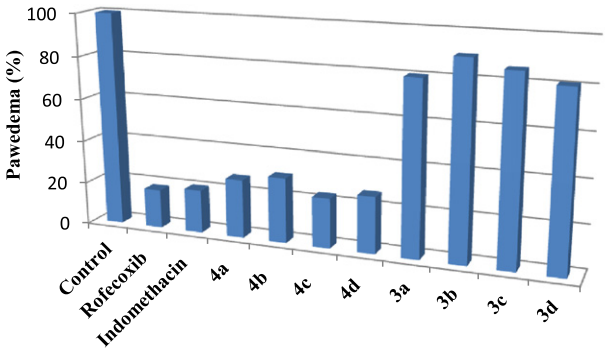

Fig. 5. Observed percentage paw edema in control, standard and test groups at 5h.

at a distance of 2.42782 Å. The nitro group of nimesulide formed hydrogen bonds with –NH of imidazole ring of His_{90} at a distance of 2.24116 Å and also formed a hydrogen bond with Arg_{513} at a distance of 2.58613 Å. The phenyl group showed a prominent π–π stacking interaction with the phenyl ring of Tyr_{355} at 1.92819 Å along with the van der Waals interactions with Val_{523} and Met_{522} at distances of 3.1028 Å and 3.35674 Å respectively.

The docking studies with compounds **4a**–**4d** suggested that one of the most important interaction of these compounds with COX-2 enzyme is hydrogen bonding of the sulphonamide oxygen with Arg_{120} as seen with nimesulide. Fig. 6 shows the hypothetical binding model for interactions of nimesulide and the test compounds **4a**, **4c** and **4d** within the COX-2 active site. A strong bonding was observed for the compounds **4c**, **4a** and **4d** at distances of 2.243 Å, 2.422 Å and 2.085 Å respectively. Interestingly, the compound with least *in vivo* efficacy i.e., **4b** formed the weakest bond with Arg_{120} at 3.2712 Å. The sulphonamide oxygen was also showing strong hydrogen bonding with Tyr_{355} in compounds **4a** and **4d** at distances of 2.096 Å and 1.853 Å respectively. These interactions were also seen for compound **4c** at a distance of 3.533 Å. These additional interactions were found to be insignificant in **4b**. The hydrogen bonding interactions of **4d** with exocyclic $-NH_2$ of His_{90} and Arg_{513} Å at distances of 3.373 Å and 1.97122 Å were quite similar to interaction of nitro group in nimesulide with the same amino acids. Incidentally, the compound with maximum *in vivo* efficacy **4a** showed much stronger (>nimesulide) bonding of the carbonyl oxygen with exocyclic $-NH_2$ of His_{90} at a distance of 1.7313 Å. Although, interactions with Arg_{513} Å were not there, additionally, the methyl group next to the carbonyl group showed strong interaction with Phe_{518} at a distance of 2.6521Å. These interactions were not seen in case of compounds **4b** and **4c** but the carbonyl group was located in the vicinity of Trp_{387} and Tyr_{385} (within a distance of 4 Å) in **4b** and in the vicinity of Trp_{387}, Tyr_{385} and Gly_{526} in **4c**. Further, the alkyl chain also showed additional van der Waals interactions with the active site in compounds **4a** and **4c**. In **4a**, the alkyl chain was interacting with Val_{523}, Tyr_{387}, Ser_{530} and Tyr_{385} at distances of 3.16965 Å, 3.03821 Å, 2.1011 Å and 2.27149 Å respectively. The alkyl chain of **4c** was located in the vicinity of the amino acids Arg_{513}, Ser_{353}, Tyr_{355}, His_{90}, Val_{523} and Gln_{192} and strong interactions were seen with Ser_{353} and His_{90} at distances of 2.01664 Å and 1.87751 Å respectively. The cyclohexyl group of **4d** was also found to show moderate interactions with amino acids Ser_{530}, Tyr_{385}, Ala_{527}, Val_{523}, Tyr_{387} and Leu_{352} within a distance of 3.8 Å. Minimum interactions of the alkyl group were seen in **4b** and alkyl group was present in the vicinity of amino acids His_{90}, Ser_{353}, Gln_{192} and Ile_{517} within a distance of 4.0 Å. The final DockScore based on overall interaction energies for the test and standard compounds is given in Table 4 and the maximum score was obtained for compounds **4a** and **4d** which had nearly similar values.

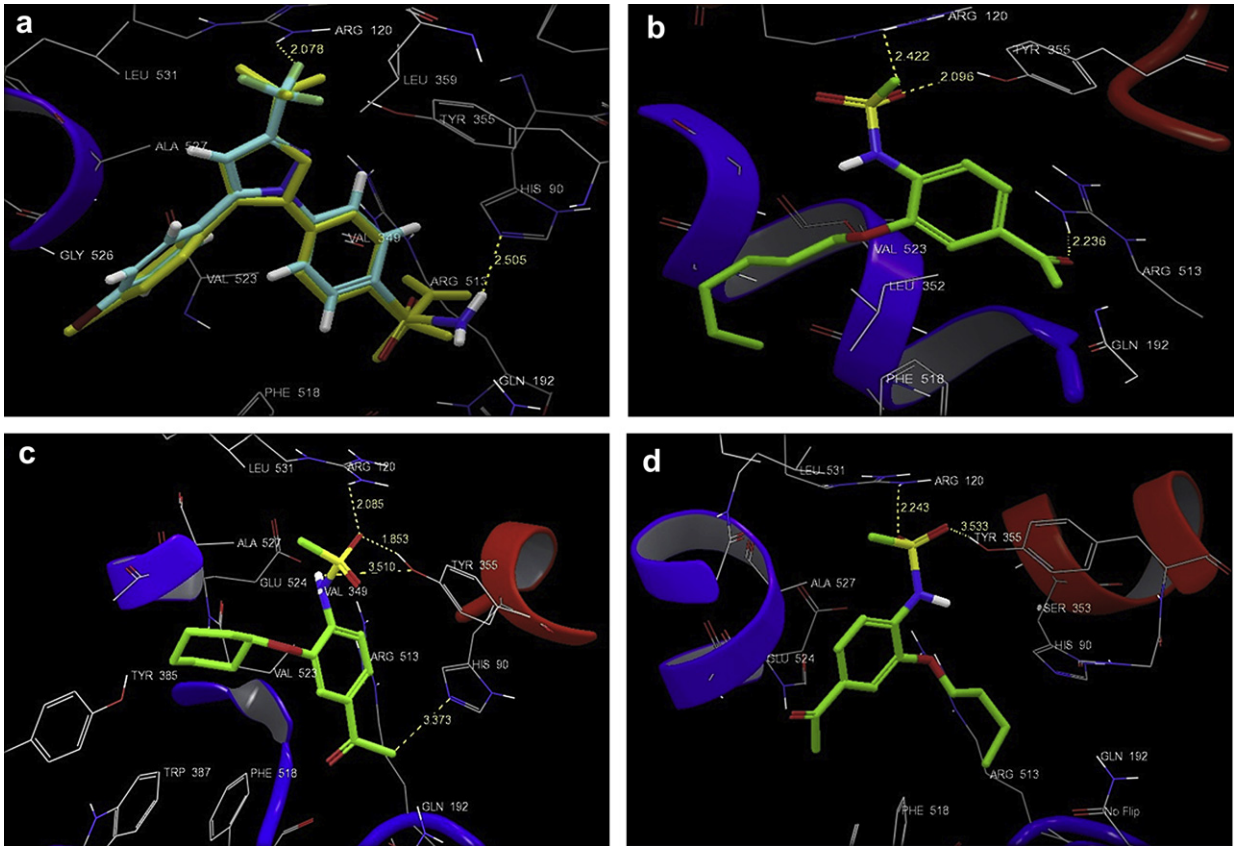

Fig. 6. Hypothetical binding model for interaction of nimesulide superimposed over SC-558 (yellow) (top left) and compounds **4a** (top right), **4c** (bottom right) and **4d** (bottom left) showing important H-bonding interactions with amino acid residues (Arg_{120}, His_{90}, Tyr_{355}) in the COX-2 active site. (For interpretation of the references to colour in this figure legend, the reader is referred to the web version of this article.)

A comparison of the docking studies with the observed pharmacological results suggests a very good correlation as the most potent test compound **4a** was also shown to dock best in the active site consisting of the amino acids Arg_{120}, His_{90}, Tyr_{385}, Tyr_{387}, Tyr_{355}, Ser_{530}, Val_{523}, and Phe_{518}. These studies particularly highlighted the importance of two features in the target compounds for COX-2 inhibition, firstly, the presence of the sulphonamide group for bonding with Arg_{120} and Tyr_{355} and secondly, the presence of carbonyl group for hydrogen bonding with His_{90}. Both these interactions were noted for the compounds **4a** and **4d** which were also seen to demonstrate the best pharmacological profile. A slightly lower activity was seen for **4c** which may be accounted for a strong (in fact, strongest amongst the tested compounds) interaction with Arg_{120} and Tyr_{355}, although, no bonding was seen with His_{90}. The least potent compound **4b** showed the weakest interaction of the sulphonamide group with Arg_{120} and Tyr_{355} and no significant interaction was seen between the carbonyl group and His_{90}. The docking studies also suggested the importance of alkyl group for COX-2 binding as the best compound (**4a**) amongst the series also demonstrated best alkyl group interactions with the active site and the least efficacious compound (**4b**) showed none at all.

Table 4
DockScore of the active compounds.

Compound No.	Dock score	Rank score
4a	55.247	1
4b	23.688	4
4c	39.156	3
4d	54.543	2
Nimesulide	92.748	Standard
SC-558	66.683	Standard

2.4.2. Computation of physicochemical parameters and ADME profiling

Table 5 lists the values of selected molecular parameters for the compounds **4a**–**4d** as well as four representative anti-inflammatory drugs having gastrointestinal tolerability. Amongst these, we included the prototypic drugs nimesulide and flosulide and two drugs belonging to the 'diaryl substituted heterocycle' category *viz* rofecoxib and celecoxib. Computation was done employing ChemBio3D Ultra version12.0 after carrying out MM2 minimization of the compound structures. Some of these parameters such as log *P*, topological polar surface area, TPSA are recognized parameters for prediction of drug transport properties. Further, steric and molecular surface descriptors, e.g., SAS, SEV and ovality and other parameters such as Molecular Topological Index MTI and Weiner Index WI were calculated.

ADME prediction methods were used to assess the bioavailability of the active compounds **4a**–**4d** and the reference drugs. Herein, we calculated the compliance of the prepared compounds to the Lipinski's 'rule of five' [19] which has been widely used as a filter for substances that could likely be further developed in drug design programs. According to this rule, poor absorption or permeation is more likely when there are more than five H-bond donors, ten H-bond acceptors, the molecular weight (MW) is greater than 500 and the calculated Log P (CLogP) is greater than 5. Molecules violating more than one of these rules may have problems with bioavailability. Further, TPSA, which is a measure of a molecule's hydrogen bonding capacity, is another key property that has been linked to drug

Table 5
Calculation of various molecular properties of synthesized compounds.

Compound	Mol. weight (MW)	Molecular refractivity (MR) cm^3/mole	Connolly solvent accessible surface area ($Å^2$)	Connolly molecular surface area ($Å^2$)	Connolly solvent excluded volume ($Å^3$)	Ovality	CLogP	Topol. polar surface area (TPSA) ($Å^2$)	Mol. Topol. Index (MTI)	Wiener Index (WI)	No. of H-bond acceptors	No. of H-bond donor NH	No. of violations LR[a]
4a	285.350	73.627	534.993	273.349	240.665	1.460	0.682	72.47	5488	742	4	1	0
4b	299.385	78.228	566.975	292.281	258.052	1.491	1.100	72.47	6524	878	4	1	0
4c	313.412	82.829	597.956	310.463	273.810	1.522	1.517	72.47	7713	1034	4	1	0
4d	311.396	80.767	520.556	277.022	271.536	1.366	0.988	72.47	6979	936	4	1	0
Nimesulide	309.310	69.128	462.837	239.576	228.221	1.320	3.08	95.71	6755	936	4	1	0
Rofecoxib	316.370	83.073	5523.556	270.378	254.249	1.393	2.148	60.44	7984	1061	4	0	0
Celecoxib	369.360	88.104	561.488	291.740	261.017	1.477	2.882	75.76	10,071	1475	7	1	0
Flosulide	351.360	86.725	543.109	285.870	261.197	1.442	2201	63.24	9129	1304	6	1	0

[a] Number of violations from lipinski's rule of five.

bioavailability. Passively absorbed molecules with a TPSA >140 are thought to have low oral bioavailability [20]. Predictions of ADME properties for studied compounds are given in Table 5. The results show that the synthesized compounds comply with these rules and the standard drugs also do not show any violation. Theoretically, these compounds should present good passive oral absorption and differences in their bioactivity may not be attributed to this aspect.

3. Conclusion

A series of 3-alkoxy-4-methanesulfonamido acetophenone derivatives have been designed based on field alignment studies with nimesulide and flosulide. The pharmacological evaluation of the synthesized compounds has shown good anti-inflammatory effect in compounds **4a**, **4c** and **4d**. *In silico* (docking studies) were done to investigate the hypothetical binding mode of the target compounds to the cyclooxygenase isoenzyme (COX-2). The results from the docking studies were found to be in good agreement with the results from pharmacological studies and suggested the importance of sulphonamido and carbonyl functions for biological activity which also explains the absence of anti-inflammatory activity in compounds **3a**–**3d**. Further, the compounds comply with Lipinski's rule of five which signifies a good absorption and hence, good bioavailability so that the observed differences in bioactivity of the compounds may be attributable to the differences in their chemical structures.

4. Experimental protocols

Infrared spectra were recorded in KBr pellets on Perkin Elmer RX 1 spectrophotometer. Proton NMR was recorded on Bruker Avance-II, 400 MHz instrument. For NMR, solutions were made in deuterated chloroform employing tetramethylsilane as internal reference. Mass spectra were obtained with Vg-11–250 J70S spectrometer at 70eV using electron ionization (EI source). For mass spectra, solutions were made in HPLC grade methanol.

4.1. Synthesis of compounds

4.1.1. 6-Acetyl benzo[d]oxazol-2-(3H)-one (*1*)

To a solution of 5.4 g (40 mmol) benzoxazolinone in 100.0 g of polyphosphoric acid, 3.6 ml (40 mmol) of glacial acetic acid was added with stirring. The mixture was heated to a temperature of 90–100 °C, and stirred at this temperature for 3 h. After cooling, the reaction mixture was added to 1000 ml of cold water. The precipitates obtained were filtered, dried and recrystallized from 95% alcohol to give pure 6-acetylbenzoxazolinone as light brown crystals. Yield 60%. m.p. 222–223 °C. UV (λ_{Max} (MeOH)) 323 nm (ϵ_{max} 50,661). FTIR (KBr, cm^{-1}): 3401, 3150, 3079, 2979, 2880, 1720, 1680, 1595, 1451, 1385, 1283, 1201, 1036, 765 and 664. ^{1}H NMR (400 MHz; $CDCl_3$, δ J): 7.51 (broad s, 1H); 7.26 (dd, 1H, $J = 6.5$ Hz, 1.7 Hz); 7.24 (d, 1H, $J = 3.0$ Hz); 7.12 (d, 1H, $J = 4.0$ Hz); 2.40 (s, 3H). MS [EI, m/z (relative intensity)]: 177 (100) [$M^{\cdot+}$].

4.1.2. 1-(4-Amino-3-hydroxyphenyl)ethanone (*2*)

To 60 ml of 10% aqueous sodium hydroxide solution in 120 ml ethanol, was added 6-acetylbenzoxazoline 5.3 g (30 mmol) and refluxing was carried out for 6 h. After cooling, the solution was acidified with concentrated hydrochloric acid and then, the saturated solution of sodium carbonate was added slowly till the effervescence ceased. The precipitates obtained were filtered, dried and recrystallized from 95% ethanol. Yield 3.84 g (85%). m.p. 168–169 °C. UV (λ_{max} (MeOH)) 331 nm (ϵ_{max} 20,940). FTIR (KBr, cm^{-1}): 3470–3372, 3130, 2922, 2852, 1680, 1508, 1460, 1404, 1260 and 755. ^{1}H NMR (400 MHz; $CDCl_3$, δ J): 7.40 (m, 2H); 7.00 (broad s,

1H); 6.90 (d, 1H, $J = 10.4$ Hz); 5.34 (broad s, 2H); 2.17 (s, 3H). MS [EI, *m/z* (relative intensity)]: 151 (100) [$M^{\cdot+}$].

4.1.3. General procedure for preparation of 1-(4-amino-3-alkoxyphenyl)ethanones (**3a**–**3d**)

To 4-amino-3-hydroxy acetophenone (30 mmol) dissolved in 21.0 ml of pyridine, 1.6 g (30 mmol) of potassium hydroxide was suspended into this solution. To the resulting viscous solution, 50 mmol of 1-bromoalkane was added and refluxing was carried out for 7–8 h. Extraction was carried out with a mixture of 1 M conc. hydrochloric acid solution and dichloromethane (100 ml, 10:90). Dichloromethane was evaporated under vaccum to give the crude 4-amino-3-alkoxy acetophenone. The crude product was recrystallized from toluene.

*4.1.3.1. 1-(4-Amino-3-butoxyphenyl)ethanone (**3a**).* Yield 40%. m.p. 86–88 °C. UV (λ_{Max} (MeOH)) 331 nm ($\in_{max}$ 11,580). FTIR (KBr, cm^{-1}): 3399, 3100, 2962, 2950, 1680, 1632, 1488, 1411, 1340, 1256, 1113, 1186, 1024 and 684. ^{1}H NMR (400 MHz; $CDCl_3$, δ J): 7.40 (d, 1H, $J = 8.1$ Hz); 7.10 (m, 2H); 4.10 (t, 2H, $J = 7.0$ Hz); 3.60 (broad s, 2H); 2.40 (s, 3H); 1.80 (quintet, 2H, $J = 7.5$ Hz); 1.40 (sextet, 2H, $J = 7.5$ Hz); 0.90 (t, 3H, $J = 7.0$ Hz). ^{13}C NMR ($CDCl_3$) δ 199.8, 146.4, 140.8, 125.4, 121.6, 117.6, 112.8, 68.4, 30.7, 24.5, 20.0, 14.9. MS [EI, *m/z* (relative intensity)]: 207 (100) [$M^{\cdot+}$]. Anal. Calcd. for $C_{12}H_{17}NO_2$: C, 69.54; H, 8.27; N, 6.76. Found: C, 69.30; H, 8.12; N, 6.45.

*4.1.3.2. 1-(4-Amino-3-pentoxyphenyl)ethanone (**3b**).* Yield 45%. m.p. 90–93 °C. UV (λ_{Max} (MeOH)) 329 nm ($\in_{max}$ 39,696). FTIR (KBr, cm^{-1}): 3380, 3150, 3025, 2926, 2854, 1660, 1496, 1453, 1400, 1258, 1042, and 695. ^{1}H NMR (400 MHz; $CDCl_3$, δ J): 7.30 (d, 1H, $J = 6.7$ Hz); 6.60 (m, 2H); 4.20 (t, 2H, $J = 6.6$ Hz); 3.60 (broad s, 2H); 2.20 (s, 3H); 1.80 (quintet, 2H, $J = 6.4$ Hz); 1.40 (m, 4H); 1.00 (t, 3H, $J = 6.6$ Hz). ^{13}C NMR ($CDCl_3$) δ 200.0, 146.1, 141.8, 125.6, 121.7, 116.9, 114.0, 70.5, 29.3, 28.6, 26.9, 23.0, 14.9. MS [EI, *m/z* (relative intensity)]: 221 (100) [$M^{\cdot+}$]. Anal. Calcd. for $C_{13}H_{19}NO_2$: C, 70.56; H, 8.65; N, 6.33. Found: C, 69.94; H, 8.22; N, 6.25.

*4.1.3.3. 1-(4-Amino-3-hexoxyphenyl)ethanone (**3c**).* Yield 50%. m.p. 94–95 °C. UV (λ_{Max} (MeOH)) 329 nm ($\in_{max}$ 39,509). FTIR (KBr, cm^{-1}): 3404, 3098, 2928, 2862, 1636, 1499, 1453, 1462, 1400, 1270, 1052 and 752. ^{1}H NMR (400 MHz; $CDCl_3$, δ J): 7.50 (d, 1H, $J = 8.0$ Hz); 6.80 (m, 2H); 4.30 (broad s, 2H); 4.00 (t, 2H, $J = 7.6$ Hz); 2.40 (s, 3H); 1.70 (quintet, 2H, $J = 7.3$ Hz); 1.40 (m, 6H); 0.90 (t, 3H, $J = 6.6$ Hz). ^{13}C NMR ($CDCl_3$) δ 199.7, 145.1, 142.0, 127.7, 120.8, 116.7, 114.0, 70.5, 29.0, 28.7, 25.9, 22.7, 19.7, 15.0. MS [EI, *m/z* (relative intensity)]: 235 (100) [$M^{\cdot+}$]. Anal. Calcd. for $C_{14}H_{21}NO_2$: C, 71.46; H, 8.99; N, 5.95. Found: C, 70.54; H, 8.30; N, 5.40.

*4.1.3.4. 1-(4-Amino-3-cyclohexyloxyphenyl)ethanone (**3d**).* Yield 40%. m.p. 98–101 °C. UV (λ_{Max} (MeOH)) 211 nm ($\in_{max}$ 31,925). FTIR (KBr, cm^{-1}): 3399, 3100, 2927, 2856, 1637, 1575, 1499, 1460, 1377, 1270, 1152, 1052 and 1050. ^{1}H NMR (400 MHz; $CDCl_3$, δ J): 7.10 (d, 1H, $J = 8.0$ Hz); 6.90 (m, 2H); 4.40 (septet, 1H); 3.60 (broad s, 2H); 2.40 (s, 3H); 2.00 (m, 2H); 1.80 (m, 2H); 1.50 (m, 3H). ^{13}C NMR ($CDCl_3$) δ 200.1, 144.8, 142.3, 127.0, 116.5, 114.3, 120.9, 79.5, 34.2, 34.2, 26.7, 24.4, 24.4, 26.0. MS [EI, *m/z* (relative intensity)]: 235 (100) [$M^{\cdot+}$]. Anal. Calcd. for $C_{14}H_{19}NO_2$: C, 72.07; H, 8.21; N, 6.00. Found: C, 71.54; H, 8.02; N, 5.86.

4.1.4. General procedure for preparation of N-(4-acetyl-2-alkoxyphenyl)methane sulfonamides (**4a**–**4d**)

To a solution of 4-amino-3-butoxy acetophenone (10 mmol) in 150.0 ml of dichloromethane, 15.0 ml pyridine and 1.5 ml methanesulfonylchloride were added. The mixture was stirred for 6 h at room temperature. It was then partitioned between water and dichloromethane. The organic layer was washed with 1 M hydrocholoric acid and then evaporated to give 3-alkoxy-4-methanesulfonamido acetophenone. The crude product was recrystallized from toluene.

*4.1.4.1. N-(4-acetyl-2-butoxyphenyl)methanesulfonamide (**4a**).* Yield 73%. m.p. 110–112 °C. UV (λ_{Max} (MeOH)) 206 nm ($\in_{max}$ 19,843). FTIR (KBr, cm^{-1}): 3372, 3100, 2922, 2852, 1680, 1508, 1460, 1411, 1370, 1122, 1256, 1036 and 803. ^{1}H NMR (400 MHz; $CDCl_3$, δ J): 8.30 (d, 1H, $J = 6.7$ Hz); 7.40 (broad s, 1H); 6.90 (m, 2H); 4.10 (t, 2H, $J = 6.6$ Hz); 3.00 (s, 3H); 2.30 (s, 3H); 1.80 (quintet, 2H, $J = 6.3$ Hz); 1.50 (sextet, 2H, $J = 5.0$ Hz); 1.00 (t, 3H, $J = 7.4$ Hz). ^{13}C NMR ($CDCl_3$) δ 199.6, 143.9, 120.9, 133.0, 127.8, 117.0, 113.7, 69.5, 43.6, 32.0, 27.2, 19.5, 14.7. MS [EI, *m/z* (relative intensity)]: 285 (12.8) [$M^{\cdot+}$], 207 (3.0) [M-$H_2C{=}SO_2$], 151(12.8) [*m/z* 207–C_4H_8] , 150 (100) [*m/z* 207–C_4H_9], 139 (2.1), 138 (23.8). Anal. Calcd. for $C_{13}H_{19}NO_4S$: C, 54.72; H, 6.71; N, 4.91. Found: C, 54.54; H, 6.42; N, 4.50.

*4.1.4.2. N-(4-acetyl-2-pentoxyphenyl)methanesulfonamide (**4b**).* Yield 63%. m.p. 113–115 °C. UV (λ_{Max} (MeOH)) 271 nm ($\in_{max}$ 19,349). FTIR (KBr, cm^{-1}): 3380, 3150, 3025, 2926, 2854, 1660, 1496, 1453, 1431, 1400, 1350, 1258, 1157, 1042 and 965. ^{1}H NMR (400 MHz; $CDCl_3$, δ J): 7.50 (d, 1H, $J = 6.7$ Hz); 7.30 (broad s, 1H); 6.70 (m, 2H); 4.10 (t, 2H, $J = 6.5$ Hz); 3.40 (s, 3H); 2.10 (s, 3H); 1.70 (quintet, 2H, $J = 7.3$ Hz); 1.40 (m, 4H); 0.90 (t, 3H, $J = 7.3$ Hz). ^{13}C NMR ($CDCl_3$) δ 199.5, 145.0, 132.3, 125.6, 120.6, 117.1, 113.7, 72.5, 43.5, 29.7, 27.8, 26.3, 22.5, 14.5. MS [EI, *m/z* (relative intensity)]: 299 (45.3) [$M^{\cdot+}$], 256 (3.9) [M - $COCH_3$], 221 (6.5) [M–CH_2SO_2], 192 (12.7) [*m/z* 256–SO_2] , 151 (12.9) [*m/z* 221–C_5H_{10}], 150 (100) [*m/z* 221–C_5H_{11}], 136 (25.1) [*m/z* 151–CH_3] , 122 (4.5) [*m/z* 151–CO]. Anal. Calcd. for $C_{14}H_{21}NO_4S$: C, 56.16; H, 7.07; N, 4.68. Found: C, 55.94; H, 6.82; N, 4.22.

*4.1.4.3. N-(4-acetyl-2-hexoxyphenyl)methanesulfonamide (**4c**).* Yield 76%. m.p. 118–120 °C. UV (λ_{Max} (MeOH)) 271 nm ($\in_{max}$ 19,349). FTIR (KBr, cm^{-1}): 3200, 3098, 2928, 2862, 1636, 1499, 1462, 1400, 1370, 1250, 1110, 1052 and 969. ^{1}H NMR (400 MHz; $CDCl_3$, δ J): 8.30 (d, 1H, $J = 8.0$ Hz); 7.70 (broad s, 1H); 6.90 (m, 2H); 4.00 (t, 2H, $J = 6.5$ Hz); 2.80 (s, 3H); 2.20 (s, 3H); 1.70 (quintet, 2H, $J = 7.3$ Hz); 1.40 (m, 6H); 0.80 (t, 3H, $J = 7.0$ Hz). ^{13}C NMR ($CDCl_3$) δ 200.0, 143.8, 142.0, 127.8, 120.4, 117.5, 114.0, 72.5, 43.2, 29.5, 28.3, 26.7, 23.0, 19.9, 14.2. MS [EI, *m/z* (relative intensity)]: 313 (79.6) [$M^{\cdot+}$], 270 (53.6) [M - $COCH_3$], 235 (38.7) [M–CH_2SO_2], 220 (16.8) [*m/z* 235–CH_3], 206 (45.0) [*m/z* 270–SO_2] , 151 (12.9), 150 (21.3) [*m/z* 235–C_6H_{13}], 136 (100) [*m/z* 220–C_6H_{12}] , 122 (5.3) [*m/z* 150–CO]. Anal. Calcd. for $C_{15}H_{23}NO_4S$: C, 57.48; H, 7.40; N, 4.47. Found: C, 57.24; H, 6.99; N, 4.45.

*4.1.4.4. N-(4-acetyl-2-cyclohexyloxyphenyl)methanesulfonamide (**4d**).* Yield 73%. m.p. 121–122 °C. UV (λ_{Max} (MeOH)) 227 nm ($\in_{max}$ 40,405). FTIR (KBr, cm^{-1}): 3399, 3100, 2927, 2856, 1637, 1575, 1499, 1460, 1400, 1360, 1270, 1115, 1052 and 950. ^{1}H NMR (400 MHz; $CDCl_3$, δ J): 7.10 (d, 1H, $J = 8.0$ Hz); 6.90 (m, 2H); 6.80 (broad s, 1H); 4.30 (septet, 1H); 3.00 (s, 3H); 2.40 (s, 3H); 2.10 (m, 2H); 1.80 (m, 2H); 1.50 (m, 3H); 1.40 (m, 2H). ^{13}C NMR ($CDCl_3$) δ 198.9, 143.8, 133.4, 127.8, 121.3, 117.4, 112.8, 78.0, 42.7, 33.8, 33.8, 26.8, 25.5, 24.5, 24.5. MS [EI, *m/z* (relative intensity)]: 311 (20.2) [$M^{\cdot+}$], 233 (38.7) [M–CH_2SO_2], 229 (35.7) [M – C_6H_{10}], 151 (34.1) [*m/z* 233–CH_2SO_2] „ 150 (100) [*m/z* 229–CH_2SO_2], 136 (18.5) [*m/z* 151–CH_3] , 122 (4.4) [*m/z* 150–CO]. Anal. Calcd. for $C_{15}H_{21}NO_4S$: C, 57.86; H, 6.80; N, 4.50. Found: C, 56.68; H, 6.17; N, 4.00.

4.2. Pharmacological evaluation

4.2.1. Anti-inflammatory activity

The anti-inflammatory activity was evaluated using *in vivo* carrageenan-induced rat paw edema model considered as the

most conventional one for acute inflammation. The wistar rats (150–200 g) of either sex were divided into 19 groups of six rats each. A mark was made on both the hind paws (right and left) just beyond tibio-tarsal junction to ensure constant paw volume. In all the groups, 0.1 ml of 1% w/v carrageenan solution was injected in the plantar region of the left paw of the rats and paw volume was noted at 0, 1, 2, 3, 4, and 5 h. In the control group, 0.5% solution of CMC was administered. In treated groups (three dose groups per compound), the test compounds were administered *p.o.* as a suspension in CMC, 30 min after the injection of carrageenan solution. Similarly, in the standard groups, rofecoxib and indomethacin were administered as a suspension in CMC *p.o.* 30 min after the injection of carrageenan solution. The paw volume was noted before treatment and after treatment at different time intervals with the help of plethysmograph by mercury displacement method. Percentage edema and percentage reduction in edema were calculated according to the formula.

$$\%\ \text{edema} = 100 - [(1 - V_t/V_c) \times 100]$$

$$\%\ \text{reduction in edema} = (1 - V_t/V_c) \times 100$$

V_t and V_c designate edema volume in drug treated and control groups

4.2.2. Evaluation of gastric ulcerogenic potential

Wistar rats of either sex weighing 150–200 g were divided into control, standard (rofecoxib and indomethacin) and various test compound groups ($n = 6$). The test compounds and indomethacin were administered orally at three dose levels. Six hours later, the animals were sacrificed by cervical dislocation and their stomachs were removed, inflated by injecting 7.0 ml 2% formalin, immersed in 2% v/v formalin solution for 10 min to fix the gastric wall, and then opened along the greater curvature. The area of each lesion that had developed in the granular mucosa was measured under a dissecting microscope with a square grid (10x), summed per stomach, and used as a lesion score. The lengths of the longest diameters of the lesions are measured and summated to give a total lesion score (in mm) for each animal, the mean count for each group being calculated.

4.3. Docking studies

The computational studies were carried out using Dell Precision workstation T3400 (Intel Core 2 Duo Processor; 4 GB RAM, 250 GB hard disk and Nvidia Quodro FX 4500 graphics card) using Accelrys-Discovery Studio-2.1 (license no. FOD 297AOA463E4AA2E34). The docking poses were taken by using GLIDE (Schrodinger Inc.) [21]. The synthesized molecules were evaluated *in silico* (docking) using the crystal structure of cyclooxygenase-2 complexed with a selective inhibitor, SC-558 (PDB Code: 1CX2) [22,23] and fitness scores were calculated with LigandFit (Accelrys-Discovery Studio-2.1) software. COX-2 enzyme contains 587 amino acids and one ferric heme group. The X-ray structure of mouse (*Musmusculus*) COX-2 has been resolved as uninhibited, as well as in the presence of four inhibitors. There is 87% sequence similarity between COX-2 enzyme from human and the mouse origin. Further, the strict conservation of the active sites in both the species [22] suggests that the structure of human COX-2 should be similar to the mouse enzyme and the mouse COX-2 may be taken as a model for the human COX-2 enzyme. The COX-2 protein exists *in situ* as a dimer but the monomer structure alone has always been considered in molecular modeling studies assuming the interactions governing the COX-2 inhibitor binding to be reproducible using one monomer. COX-2 crystallizes with each monomer consisting of three independent folding units: an N-terminal epidermal growth factor domain (EGF), a membrane-binding motif and a C-terminal catalytic domain, which contains the active cyclooxygenase and peroxidase active sites. Out of the structures lodged in the PDB, 1CX2 was selected as it contains a COX-2 selective inhibitor SC-558 bound to the enzyme and the same could be employed as a validation system also.

4.3.1. Protein preparation

The crystal structure of cyclooxygenase-2 complexed with SC-558 was taken from the Protein Data Bank (PDB Code: 1CX2) and prepared using Schrodinger protein preparation wizard tool. Hydrogen atoms were added to the crystal structure. As a pre-processing step, the water molecules, bound ligand and cofactors were removed from the template. The protein was subjected to minimization using the CHARMm force field implemented in Accelrys-Discovery studio-2.1. The minimization iterations were set at 1000 steps and minimization gradient tolerance of 0.001.The prepared structure was saved in mol2 file format.

4.3.2. Preparation of ligands

All ligand 2D structures were built in ISIS Draw and then transferred to Accelrys-Discovery Studio-2.1. After selection of ligand hydrogen atoms were added. The ligands were subjected to minimization using the CHARMm force field and prepared by using 'prepare ligands' module of Accelrys-Discovery Studio-2.1. The prepared ligands were saved as mol2.

4.3.3. Docking

The ligand conformations were generated using LigandFit Monte-Carlo techniques which were subsequently docked into the active site using a shape-based initial docking. The docked poses were minimized using CHARMm force field followed by generation of docking scores for the same. Simulations were performed with 1000 iterations. A grid resolution was set to 0.5 A° (default), and the ligand-accessible grid was defined such that minimum distance between a grid point and the protein is 2.0 A° for hydrogen and 2.5 A° for heavy atoms. The grid extends from the defined active site to a distance of 3.0 A° in all directions. For analysis of docking, surface was created around the ligand molecule and then receptor-ligand hydrogen bonds were measured. Dockscore, LigScore1, LigScore2, PLP1, PLP2, Jain and PMF scores were calculated for all the conformations of the ligands to evaluate the fitness score relationship with its biological activity.

4.4. Field align studies

The three dimensional and field similarity of the compound set with respect to standard drugs was assessed using *FieldAlign2.1.1*™ (Cresset BioMolecular Discovery Ltd., UK). The reference drugs nimesulide, flosulide, rofecoxib and celecoxib were imported from ChemBioDraw Ultra 12.0 in sdf (MDL mol) format. Molecules to be aligned were imported in 2D from ChemBioDraw Ultra 12.0 as sdf (MDL mol) files. The maximum number of conformations generated for any molecule was limited to 200 in order to have a balance of the quality of alignments and calculation time. Number of high temperature dynamics for flexible rings was set at 5. Gradient cut-off for conformer minimization was 0.5. Coarseness of the sampling of conformational space was controlled by filtering duplicate conformers at rms 0.5. Standard scoring function was used based on 50% shape similarity and 50% dice volume similarity to derive overall similarity between two conformations. Statistical analysis of the similarity results for the test compounds was done by comparison of different drug groups by All Pairwise Multiple Comparison test (Tukey Test) ($p < 0.05$) (Jandel Sigmastat version 2.0).

Acknowledgments

The research grant provided by the University Grants Commission is duly acknowledged.

References

[1] R.F. Borne, Non-steroidal anti-inflammatory drugs, in: D.A. Williams, T.L. Lemke (Eds.), Foye's Principles of Medicinal Chemistry, fifth ed, Lippincott Williams & Wilkins, New York, 2002, pp. 751–793.
[2] D.B. Mc-Namara, P.R. Mayeux, Nonopiate analgesics and anti-inflammatory drugs, in: P.L. Munson, R.A. Muller, G.R. Breese (Eds.), Principles of Pharmacology: Basic Concepts and Clinical Applications, third ed, Int. Thomson Publishing Co., Chapman & Hall, New York, 1995, pp. 1160–1178.
[3] A. Blazovics, K. Hagymasi, L. Pronai, Orv. Hetil. 145 (2004) 2523–2529.
[4] C.D. Funk, Science 5548 (2001) 1871–1875.
[5] C.E. Eberhart, R.N. Dubois, Gastroenterology 109 (1995) 285–301.
[6] J.J.F. Belch, J. Biol. Chem. 36 (1989) 219–234.
[7] J.S. Bennet, A. Daugherty, D. Herrington, P. Greenland, H. Roberts, K.A. Taubert, Circulation 111 (2005) 1713–1716.
[8] J.R. Vane, R.M. Botting, J. Rheumatol. Suppl. 102 (1996) 9–21.
[9] G. Green, Clin. Cornerstone 5 (2001) 50–60.
[10] H.E. Vonkeman, M.A. van de Laar, Semin. Arthritis Rheum. 39 (2010) 294–312.
[11] M.C. Allison, A.G. Howatson, C.J. Torrance, F.D. Lee, R.I.G. Russell, N. Engl. J. Med. 327 (1992) 749–754.
[12] V.F. Trewin, C.J. Lawrence, S.A. Rae, G.B.A. Veitch, J. Clin. Pharm. Ther. 19 (1994) 209–214.
[13] C. Kneitz, H.P. Tony, K. Kruger, Internist (Berl) 47 (2006) 533–534.
[14] F. Wuest, X. Tang, T. Kniess, J. Pietzschand, M. Suresh, Bioorg. Med. Chem. 17 (2009) 1146–1151.
[15] W.J. Close, B.D. Tiffany, M.A. Spielman, J. Am. Chem. Soc. 71 (1949) 1265–1268.
[16] C.A. Winter, E.A. Risely, G.W. Nuss, Proc. Soc. Exp. Biol. 111 (1962) 544–547.
[17] R. Huff, P. Collins, S. Kramer, K. Seibert, C. Koboldt, S. Gregoryand, P. Isakson, Inflamm. Res. 44 (1995) S145–S146.
[18] J.L.M. Tributino, C.D. Duarte, R.S. Corrêa, A.C. Doriguetto, J. Ellena, N.C. Romeiro, N.G. Castro, A.L.P. Miranda, E.J. Barreiro, C.A.M. Fraga, Bioorg. Med. Chem. 17 (2009) 1125–1131.
[19] C.A. Lipinski, F. Lombardo, B.W. Dominy, P.J. Feeney, Adv. Drug Deliv. Rev. 46 (2001) 3–26.
[20] D.E. Clark, S.D. Pickett, Drug Discov. Today 5 (2000) 49–58.
[21] (a) Maestro, Version 9.1, Schrödinger, LLC, New York, NY, 2010;
(b) A.F. Richard, L.B. Jay, B.M. Robert, A.H. Thomas, J.K. Jasna, T.M. Daniel, P.R. Matthew, H.K. Eric, S. Mee, K.P. Jason, E.S. David, F. Perry, S.S. Peter, J. Med. Chem. 47 (2004) 1739–1749.
[22] R.G. Kurumbail, A.M. Stevens, J.K. Gierse, J.J. McDonald, R.A. Stegeman, J.Y. Pak, D. Gildehaus, J.M. Miyashiro, T.D. Penning, K. Seibert, P.C. Isakson, W.C. Stallings, Nature 384 (1996) 644–648.
[23] E. Filipponi, V. Cecchetti, O. Tabarrini, D. Bonelli, A. Fravolini, J. Comput. Aided Mol. Des. 14 (2000) 277–291.